

# A simulation on microstructure sensitivity to very-high-cycle fatigue behavior of metallic materials

Zhengqiang Lei, Jijia Xie, Aiguo Zhao, Youshi Hong\*

*State Key Laboratory of Nonlinear Mechanics (LNM), Institute of Mechanics, Chinese Academy of Sciences, Beijing 100190, China*

Received 22 July 2010; revised 27 July 2010; accepted 30 July 2010

---

## Abstract

This paper studied the microstructure sensitivity to very-high-cycle fatigue of metallic materials based on Tanaka and Mura model by using Monte-Carlo method. In this simulation, local stress, frictional stress and inclusion size are assumed to be random variables, and two sensitivity indicators are proposed: sensitivity of mean value and sensitivity of standard deviation. Results indicate that fatigue failure is most sensitive to frictional stress, and the dispersity of variables also influences the fatigue life.

© 2010 Published by Elsevier Ltd. Open access under [CC BY-NC-ND license](#).

**Keywords:** very-high-cycle fatigue; Tanaka and Mura model; microstructure sensitivity; Monte-Carlo simulation; metallic materials

---

## 1. Introduction

Under hydrodynamic actions, such as water currents, waves and tides, supporting system of Submerged Floating Tunnels (SFT) endurances a fluctuated tensile stress in water [1], and the design life is over fifty years, so fatigue failure under hydration medium environment can not be neglected for the design of anchor rope. Very-high-cycle fatigue (VHCF) is the study of fatigue failure behaviors of materials and structures beyond and equal to hundreds millions of cycles [2]. A number of experimental data has been accumulated and experimental phenomenon has been reported during the research of VHCF of metallic materials in recent years. Especially for high strength steels, it is often shown a step-wise  $S-N$  curve [3, 4], the plateau present to the region of  $10^5$  to  $10^7$  cycles. The plateau of the  $S-N$  curve, i.e. the transition stress at which the crack initiation changes from surface to subsurface is the traditional fatigue limit. When the nominal stress is bellow the traditional fatigue limit, fatigue failure occurs in the VHCF ( $N > 10^7$ ) region. This is a new challenge to the design of long life components. Qian et al. [5] showed that the fatigue strength of the steel in water was remarkably degraded compared with that in air and the fatigue strength in 3.5% NaCl solution was even lower than that in water. Therefore, it is necessary to further understand the fatigue behavior of very high strength steels, which may be used in the SFT supporting system.

---

\* Corresponding author. Tel.: +86-10-82543966; fax: +86-10-62561284.  
E-mail address: hongys@imech.ac.cn

According to the present research situation, the fatigue failure is divided into two stages: crack initiation stage and crack propagation, and the crack initiation control the fatigue life of VHCF [6]. Fatigue life is influenced by many factors at different stages. Surface roughness [7], material strength, loading frequency, loading environment [8], inclusion size [6] and distribution play an important part in determining the VHCF life. Tanaka and Mura [9] proposed a micromechanical model for estimating the fatigue life of metallic materials. In their model, local shear stress, frictional stress and characteristic size of microstructure were important parameters in fatigue crack initiation.

The principal objective of this work is to show the scatter of fatigue life and microstructures sensitivity of VHCF of metallic materials based on Tanaka and Mura model by Monte-Carlo analysis.

## 2. Fatigue crack initiation model

### 2.1. Crack initiation model

Tanaka and Mura [9] model has been widely used to fatigue crack initiation life prediction [10–12]. It can be simplified as

$$N_i = \frac{AW_s}{(\Delta\tau - 2k)^2} \quad (1)$$

where  $N_i$  is the cycles to crack initiation,  $W_s$  is the specific fracture energy,  $\Delta\tau$  is the range of local shear stress,  $k$  is frictional stress.  $A$  is a function depending on the materials properties and the type of initial cracks. Three types of initial cracks have been proposed, they are crack initiates along slip bands, crack initiates along grain boundary, and cracks initiates along the interface of inclusion. In this paper, the third type is proposed, and  $A$  has the following form:

$$A = \frac{4G(G + G_i)h^2}{G_i(h + l)^2 a_i} \quad (2)$$

where  $G$  is the bulk shear modulus of matrix,  $G_i$  is the shear modulus of inclusion,  $l$  is the semi-length of slip band,  $h$  is the semi-minor length of the elliptical slip band area,  $a_i$  is the inclusion size.

A physical interpretation of the Von Misses yield criteria is that yielding occurs when the resolved shear stress on the octahedral plane exceeds the octahedral shear strength, where

$$\tau_0 = \frac{\sqrt{2}}{3} \sigma_0 \quad (3)$$

where  $\sigma_0$  is the yield strength from uniaxial tensile test. The relationship between the shear stress amplitude and the applied stress amplitude can be defined as [6]:

$$\Delta\tau = \frac{\sqrt{2}}{3} \Delta\sigma \quad (4)$$

Using Griffith crack theory we can calculate the  $W_s$  as follows [13]:

$$W_s = \frac{\Delta K_{th}^2}{2E} \quad (5)$$

where  $\Delta K_{th}$  is the fatigue crack growth threshold, its value is determined by the three points notch test done by Qu et al. [14].

In this paper, the following assumptions are made:

- (1) The life of fatigue crack propagation is ignored, so the fatigue crack initiation life is considered to be the whole fatigue life.
- (2) The semi-length of slip band is assumed to be equal to the semi-minor length of the elliptical slip band area.
- (3) The shear modulus of inclusion is assumed to be equal to the bulk shear modulus.

## 2.2. Primitive random variables

### 2.2.1. Local stress

In rotation bending fatigue test, local stress is changed along radius direction, so inclusion at different location has different stress. Experiment results show that the maximum depth of inclusion where crack initiates is about 250 microns [15] away from surface of the materials, so the local stress around inclusion where fatigue cracks initiate is close to the maximum stress with a small fluctuation. Here local stress is assumed to follow a normal distribution with a Coefficient of Variation (COV) of 0.1.

### 2.2.2. Inclusion size

In order to research the influence of the inclusion size on the fatigue limit, Murakami et al. [16] used the parameter  $\sqrt{\text{area}}$  to remark the inclusion size and got satisfying prediction result. Now it is widely accepted in VHCF study. Inclusion size is mainly influenced by productive technology, Murakami used Gumbel distribution to manifest the maximum size of the inclusion, but few data can be found about the distribution of inclusion size. Here we assume the normal distribution with a COV of 0.3.

### 2.2.3. Frictional stress

The variation in frictional stress depends on the interaction between mobile dislocations and sub-grain obstacles. Only a few papers can be found about the determination of the value of frictional strength. Wang et al. [4] deduced a new expression that the frictional strength of high strength steel was about a quarter of fatigue limit at stress ratio  $R=-1$ . Tanaka [17] indicated that a two-parameter Weibull distribution with a COV between 0.3 and 0.7 can be used to describe the frictional stress. In the present paper, the mean frictional strength is derived from fatigue limit and a two-parameter Weibull distribution with a COV of 0.3 will be used.

## 3. Computational method

Here a structure reliability method [18] will be used for fatigue failure possibility analysis. The reliability of the crack initiation life  $R$  is defined as the probability that the crack initiation life  $N(X)$  will exceed a specified number of cycles  $N_s$ .  $R$  is determined using the performance function defined as:

$$g(X) = N(X) - N_s \quad (6)$$

in direct Monte-Carlo simulation method.  $N(X)$  is determined by Tanaka and Mura model.

Monte-Carlo method begins with sampling of all random variables, and then the value of the performance function is solved for further probability analysis. To the present problem, a vector  $X$  will be generated firstly, where  $X$  is a vector of three random variables  $\Delta\sigma, k, a_i$ . Then the value of  $g(X)$  can be obtained. Repeat this process  $N$  times, if  $N$  is large enough, the probability of  $g(X) < 0$  will be equal to the frequencies of  $g(X) < 0$  according to the law of large numbers, thus we obtain the fatigue failure probability  $P_f = 1 - R$ .

Cumulative Distribution Function (CDF)  $P_f$  of a response  $g$  can be represented as

$$P_f = P(g(X) < 0) = \int \dots \int_{\Omega} f_X(x) dx \quad (7)$$

where  $f_X$  is the probability density function of  $X$ ,  $\Omega$  is the domain in  $X$  which satisfy the performance function constraint  $g(X) < 0$ . Based on integral in Eq. (7), sampling based CDF sensitivities of  $P_f$  with respect to a distribution parameter  $\theta$  (mean or standard deviation of  $X$ ) can be defined as

$$\frac{\partial P_f}{\partial \theta} = \int \dots \int_{\Omega} \frac{\partial f_x}{\partial \theta} dx \quad (8)$$

$\partial P_f / \partial \theta$  presents the change in CDF due to the change in a statistical meaning that characterizes the distribution function of the input variable  $X$ . Eq. (8) can be presented by an expectation function:

$$\frac{\partial P_f}{\partial \theta} = \int \dots \int_{\Omega} \frac{P_f \cdot \partial f_x}{f_x \cdot \partial \theta} \left( \frac{f_x}{P_f} \right) dx = E \left[ \frac{P_f \cdot \partial f_x}{f_x \cdot \partial \theta} \right]_{\Omega} \quad (9)$$

in which  $P_f$  is the probability in the  $\Omega$  domain and  $f_x/P_f$  is the sampling density function in  $\Omega$  which is now the sampling domain. Based on Eq. (9) the mean sensitivity  $S_{\mu_i}$  and the standard-deviation sensitivity  $S_{\sigma_i}$  are defined as [19]:

$$S_{\mu_i} = \frac{\partial P_f / P_f}{\partial \mu_i / \sigma_i} \quad (10)$$

$$S_{\sigma_i} = \frac{\partial P_f / P_f}{\partial \sigma_i / \sigma_i} \quad (11)$$

where  $\mu_i$  and  $\sigma_i$  are respectively the mean and the standard deviation of the random variable  $X_i$ .

For independent variables, the joint probability density function (PDF) of  $X$  is a product of the PDF of  $X_i$ , Eq. (4) can be simplified to

$$\frac{\partial P_f / P_f}{\partial \theta_i / \sigma_i} = E \left[ \frac{\sigma_i \partial f_x}{f_x \partial \theta_i} \right]_{\Omega} = E \left[ \frac{\sigma_i}{f_x} \frac{\partial f_{x_i}}{\partial \theta_i} \frac{\partial f_x}{\partial f_{x_i}} \right]_{\Omega} = E \left[ \frac{\sigma_i}{f_{x_i}} \frac{\partial f_{x_i}}{\partial \theta_i} \right]_{\Omega} \quad (12)$$

Eq. (12) is a function of only the variable  $X_i$  and its probability distribution parameters  $\theta_i$ . It can be simplified further by transform the non-normal variables  $X$  to standard normal variables  $U$  using the following transformation:

$$U_i = \Phi^{-1} \left( F_{X_i} (X_i) \right) \quad (13)$$

where  $\Phi^{-1}(\cdot)$  is the inverse standard normal CDF and  $U_i$  is a normal variable with zero mean and unit standard deviation using  $U_i$  variables. Thus we can get

$$S_{\mu_i} = \frac{\partial P_f / P_f}{\partial \mu_i / \sigma_{U_i}} = E [U_i]_{\Omega} \quad (14)$$

$$S_{\sigma_i} = \frac{\partial P_f / P_f}{\partial \sigma_i / \sigma_{U_i}} = E [U_i^2]_{\Omega} - 1 \quad (15)$$

where the expectations are only over the reduced subspace defined by  $\Omega$ ,  $\mu_{U_i}$  is the mean of  $U_i$  with a nominal value of zero and  $\sigma_{U_i}$  is the standard deviation of  $U_i$  with a nominal value of one. The algorithm mentioned above is compiled and performed by MATLAB program.

## 4. Computational result

### 4.1. Fatigue failure probability

The predicted distribution of the fatigue failure probability is shown in Fig. 1 using Eq. (1) by direct Monte Carlo simulation. The bulk shear modulus  $G$  and the specific fracture energy  $W_s$  are assumed to be deterministic variables with values 79GPa and 214kN/m respectively where the value of  $W_s$  is obtained from Eq. (5). The local stress  $\sigma_s$ , frictional strength  $k$  and inclusion size  $a_i$  are assumed to be random variables. The local stress  $\sigma_s$  is normally distributed a COV of 0.1 at three stress level (mean stress): 1600MPa, 1400MPa and 1200MPa. The frictional strength is a Weibull distribution with a mean value of 500MPa and a COV of 0.3. The inclusion size is normally distribution with a mean value of 15 microns and a COV is 0.3.

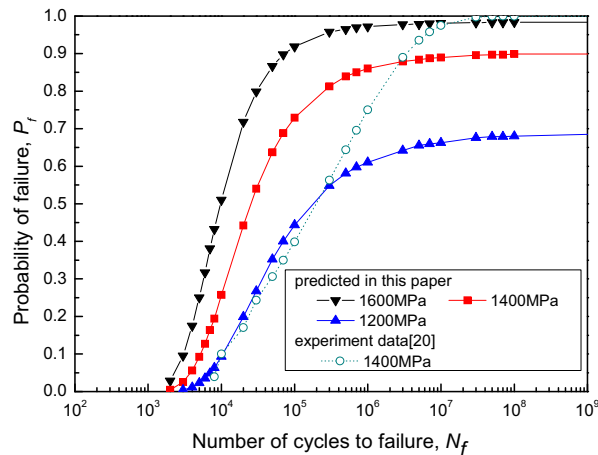


Fig. 1. Fatigue life distribution prediction at different stress level

Fig. 1 shows the change of probability of failure with the loading cycles under different local stress level. In this figure, with the increase of the stress level, the probability of failure increased at the same fatigue life, and failure probability converges to a certain value at each stress level. The convergence value also increased with the increase of the stress. For the failure probability at 1200MPa converges to 0.69 as  $N_f$  increases, this is because fatigue life can reach a infinite value when the local stress is close to the frictional stress in Tanaka and Mura model, and it is inevitable that a portion of sample values occur in this domain in the statistical analyses.

The predicted result is compared to experimental data. The shape of the failure probability curve is similar to the statistical result which is obtained by fitting the rotating bending fatigue test data through a three parameters Weibull distribution provided by Sakai research group [20], although the failure probability is some different from experiment data.

### 4.2. S-N scatter property prediction

Fig. 2 is the predicted S-N curve with the probabilistic scatter bars at four stress levels. Taking no account of small probability event, the left point at each stress level is the 2.5% fatigue failure probability point, the middle point is the mean fatigue life point and the right point is the 97.5% fatigue failure probability point or the beginning convergence point.

Fig. 2 indicates that both the mean fatigue life and the scatter of S-N curve increase with the stress decrease. Fatigue life of metallic materials ranges from  $10^4$  to nearly  $10^8$  at a certain stress level, and the mean value of fatigue life reaches  $10^9$  at 1000MPa, this means that specimen at this stress level is likely to reach an infinite fatigue life, this is similar to SUJ2 steel experiment data [20].

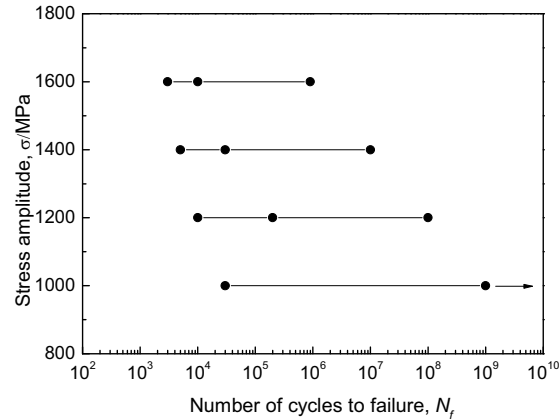
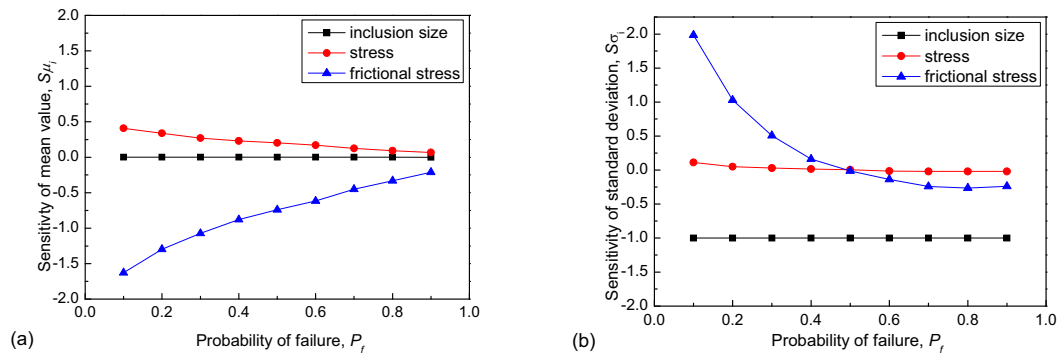


Fig. 2. Probabilistic stress versus life plot

#### 4.3. Microstructure variable sensitivity to fatigue failure

This reliability and sensitivity analysis reflects the quantitative influence of mean value and standard deviations of variables on the fatigue failure probability. Besides the variation trend of fatigue failure probability can be obtained by checking the sign of  $S_{\mu_i}$  and  $S_{\sigma_i}$  [21].

Fig. 3. (a) Sensitivity of mean value ( $S_{\mu_i}$ ); (b) Sensitivity of standard deviation ( $S_{\sigma_i}$ )

Sensitivity analysis results in Fig. 3 are calculated with local stress mean value of 1400MPa, and other conditions are as same as these in fatigue failure probability analysis. Fig. 3 shows that mean value sensitivities of stress and frictional stress are at same order of magnitude throughout the regime, and fatigue failure being most sensitive to frictional stress, then the local stress and inclusion size. It is noteworthy that inclusion size almost has no effect to the sensitivity to fatigue failure in Fig. 3, in another words influence of inclusion size is much less than influence of frictional stress and local stress. From the sign of  $S_{\mu_i}$ , it seems that the sensitivity to fatigue failure increases with increasing frictional strength, and on the contrary, it decreases with increasing local stress. From the sign of  $S_{\sigma_i}$ , the sensitivity will be enhanced by decreasing dispersity of local stress or frictional strength, or by increasing dispersity of inclusion size.

## 5. Conclusions

Direct Monte-Carlo simulation in reliability analysis is used to fatigue failure probability evaluation in this paper, and local stress, frictional stress, inclusion size are assumed to be random variables. For the problem of estimating fatigue failure possibilities and fatigue life scatter, Tanaka and Mura model is well performed in Monte-Carlo simulation. The main results are as follows:

- (1) With the increase of the stress level, the probability of failure increased at the same fatigue life, and failure probability converges to a certain value at each stress level. Both the mean fatigue life and the scatter of  $S-N$  curve increases with the decrease of stress.
- (2) Fatigue failure is sensitive to microstructures. According to sensitivity the ranking order of the three variables are frictional stress, local stress, and inclusion size. The sensitivity increases with increasing frictional strength, and on the contrary, it decreases with increasing local stress. Also the sensitivity will be enhanced by decreasing dispersity of local stress or frictional strength, or by increasing dispersity of inclusion size.
- (3) Anchor rope of SFT will endurance a fluctuated stress up to  $10^7$  cycles, so metallic materials with high frictional stress or fewer inclusions will suitable for the anchor rope considering very high cycle fatigue property of the materials.

## Acknowledgements

This paper is supported by National Natural Science Foundation of China (Grant nos. 10532070, 10772178) and Knowledge Innovation Program of Chinese Academy of Sciences (Grant no. KJCX2-YW-L07).

## References

- [1] Mazzolani FM, Landolfo R, Faggiano B, Esposto M, Perotti F, Barbella G. Structural analyses of the submerged floating tunnel prototype in Qiandao Lake (P.R. of China). *Advances in Structural Engineering* 2009; 11:439–54.
- [2] Mayer H, Haydn W, Schuller R, Issler S, Furtner B, Bacher-Höchst M. Very high cycle fatigue properties of bainitic high carbon–chromium steel. *International Journal of Fatigue* 2009; 31:242–9.
- [3] Naito T, Ueda H, Kikuchi M. Observation of fatigue fracture surface of carburized steel. *Journal of Society Materials Science* 1983; 32: 1162–66.
- [4] Sakai T, Sato Y, Oguma N. Characteristic S–N properties of high-carbon–chromium-bearing steel under axial loading in long-life fatigue. *Fatigue & Fracture of Engineering Materials & Structures* 2002; 25: 765–73.
- [5] Qian GA, Hong YS. Effect of environmental media on high cycle and very-high-cycle fatigue behaviors of structural steel 40Cr. *Acta Metallurgica Sinica* 2009; 45: 1356–63.
- [6] Wang QY, Bathias C, Kawagoishi N, Chen Q. Effect of inclusion on subsurface crack initiation and gigacycle fatigue strength. *International Journal of Fatigue* 2002; 24: 1269–74.
- [7] Itoga H, Tokaji K, Nakajima M, Ko HN. Effect of surface roughness on step-wise S–N characteristics in high strength steel. *International Journal of Fatigue* 2003; 25: 379–85.
- [8] Hong Y, Zhao A, Qian G. Essential characteristics and influential factors for very-high-cycle fatigue behavior of metallic materials. *Acta Metallurgica Sinica* 2009; 45: 769–80.
- [9] Tanaka K, Mura T. A dislocation model for fatigue crack initiation. *ASME J App Mech* 1981; 48: 97–103.
- [10] Murakami Y, Nomoto T, Ueda T, Murakami Y, Ohori M. Analysis of the mechanism of superlong fatigue failure by optical microscope and SEM/AFM observations. *Journal of the Society of Materials Science* 1999; 48: 1112–7.
- [11] Tryon RG, Cruse TA. A reliability-based model to predict scatter in fatigue crack nucleation life. *Fatigue & Fracture of Engineering Materials & Structures* 1998; 21: 257–67.
- [12] Tryon RG, Animesh D, Ganapathi K, Chandran KS. Identifying sensitive parameters at fatigue crack nucleation sites using microstructural simulation models. *The Minerals, Metals & Materials Society* 2006, p. 298–305.
- [13] Anderson TL. *Fracture mechanics, fundamental and application*. Boca Raton, FL: CRC Press; 1991.
- [14] Qu S. Study on the fatigue strength factor and the threshold of bearing steel. *Material for Mechanical Engineering* 1998; 22: 16–7.

- [15] Suh CM, Kim JH. Fatigue characteristics of bearing steel in very high cycle fatigue. *Journal of Mechanical Science and Technology* 2009; 23: 420–5.
- [16] Murakami Y, Yokoyama NN, Nagata J. Mechanism of fatigue failure in ultralong life regime. *Fatigue & Fracture of Engineering Materials & Structures* 2002; 8: 735–25.
- [17] Tanaka K, Kinefuchi M, Yokomaku T. Modeling of statistical characteristics of the propagation of small fatigue cracks. In: Miller KJ, Rios ER, editors. *Short Fatigue CracksESIS 13*, London: Mechanical Engineering; 1992, p.351–368.
- [18] Wu YT, Millwater HR, Cruse TA. An advanced probabilistic structural analysis method for implicit performance functions. *AIAA Journal* 1990; 28: 1663–9.
- [19] Wu YT, Mohanty S. Variable screening and ranking using sampling-based sensitivity measures. *Reliability Engineering and System Safety* 2006; 91: 634–47.
- [20] Sakai T et al. Statistical duplex S–N characteristics of high carbon chromium bearing steel in rotating bending in very high cycle regime. *International Journal of Fatigue* 2010; 32: 497–504.
- [21] Song SF, Lv ZZ. Structural reliability sensitivity analysis method based on Markov Chain Monte Carlo subset simulation. *Journal of Mechanical Engineering* 2009; 45: 33–8.